Journal of Building Engineering 58 (2022) 105035

Contents lists available at ScienceDirect

Journal of Building Engineering

journal homepage: www.elsevier.com/locate/jobe

Pareto principle-based advanced exergetic evaluation of geothermal district heating system: Simav case study

Oguz Arslan [a,*], Asli Ergenekon Arslan [b]

[a] Mechanical Engineering Department, Engineering Faculty, Bilecik Seyh Edebali University, Bilecik, Turkey
[b] Quality Control in Manufacturing Programme, Mechanics and Metal Technologies Department, Vocational School, Bilecik Seyh Edebali University, Bilecik, Turkey

ARTICLE INFO

Keywords:
Advanced exergy
District heating
Geothermal
Pareto principle

ABSTRACT

Geothermal energy has been used in district heating systems for many years. In these old-fashion systems, the heat of geothermal fluid is transferred to secondary fluid (water) by pipes, pumps, and heat exchanger systems. Although these systems have an easy engineering structure, the efficient use of the geothermal source is deficient depending on the thoughtless installations. In this regard, the operating parameters such as temperature and operations provided against the losses such as insulation are much more important; however, the limits of these treatments are not definite. In this regard, advanced exergy analysis is a useful tool since it takes the systems' real, unavoidable, and ideal cases into consideration through conventional exergy analysis. So, the advanced exergy method enables the determination of the improvement potential of the systems. In the advanced exergy method, the unavoidable conditions are decisive factors that should be determined, taking the economic, technological, and available thermodynamic factors into account. Pareto principle can be an alternative solution to determine the unavoidable conditions. Pareto principle indicates that 80% of the impact is sourced from the 20% potential cause. Therefore, according to Pareto principle, it is available to increase benefits by 80% through a change of 20% in the technical parameters. In this study, the advanced exergy method was conducted for the whole Simav geothermal district heating system. The unavoidable conditions were determined based on Pareto principle. According to the analysis, the highest avoidable exergy destruction ratio was determined as 8.14% for the production (well) field, where the total was 19.96%. In conclusion, an improvement potential of 10.33% was determined for the overall system.

1. Introduction

Geothermal energy is one of the most popular renewable energy sources. It is widely used in energy systems, from heating to power generation. Depending on its stable conditions, geothermal energy use for heating is widely preferred in district heating systems. In these systems, the heat of geothermal fluid is transferred to network circulating water and then is transferred to heating circuit water. During this process, the transmission pipes, the primary heat exchangers, and the substation heat exchangers are the critical components in which the heat and pressure losses occur [1,2]. There are many studies about geothermal district heating systems (GDHSs) in the literature. In these studies, GDHS were evaluated thermodynamically for performance evaluation. In addition, in some of them,

* Corresponding author.
E-mail address: oguz.arslan@bilecik.edu.tr (O. Arslan).

https://doi.org/10.1016/j.jobe.2022.105035
Received 20 March 2022; Received in revised form 1 June 2022; Accepted 23 July 2022
Available online 2 August 2022

the integration with different systems and/or different sources was evaluated for performance improvement. In Table 1, a summary of the literature is given.

According to Table 1, the exergy efficiencies range between 43.59% and 76.92%. The exergy efficiency of Afyon GDHS was raised from 47.54% to 60.63%, with an increase of 27.5% by just renovation of the pipes of the transmission line [4,5]. Also, it is possible to increase the exergy efficiency by boosting the GDHS with technological systems such as heat pumps. For example, it is possible to increase the exergy efficiency of Simav GDHS from 43.77 to 76.92 by integrating a large-scale heat pump into the heat center [2,7]. It was reported that it is available to increase exergy efficiency at a rate of 7.4%–9% by small-scale heat pump integration [8,9]. Through heat pump integration, it is possible to save the primary heat supply of geothermal resources [6]. Also, multi-purposed systems would undoubtedly increase the efficient use of geothermal resources [10–12]. For instance, it is possible to get an exergy efficiency of 65.75% for Simav GDHS, whereas it is just about 43.77% for single-use [2,10]. It is also available to integrate geothermal energy with different sources such as waste heat and solar [13–15]. Although several studies offer methods of improving the GDHS efficiency by energy and exergy methods, they are not sufficient to determine the limits of improvement. They are confused about evaluating the single systems in comparison.

In this regard, advanced exergy analysis is a potential tool for analyzing district heating systems. The advanced exergy method is also precious since it determines the endogenous and exogenous parts of exergy destructions and the improvement potential of the system. In the literature, limited studies were conducted about the analysis of GDHSs through advanced exergy. A comparative literature review for GDHSs is given in Table 2.

According to Table 2, the advanced exergy analysis results show that it is possible to increase the exergy efficiency of a GDHS at a rate ranging between 3.07% and 54.64%. However, these improvements were obtained under unavoidable conditions of $\Delta T = 0.5–1\ ^{\circ}C$, $\eta = 0.98$, and $\Delta P = 10$ kPa. These conditions include the extreme cases where they are available for relatively larger or limited systems.

In this regard, the unavoidable and ideal conditions were critical for determining the improvement potential of any energy system such as GDHS since this potential is directly related to unavoidable conditions determined by the experts [20–22]. In this regard, it is crucial to determine the realistic unavoidable conditions for achieving practical system improvement. So, in this study, Pareto principle was embedded in the advanced exergy analysis.

According to Table 2, the conducted advanced exergy analyses in the literature were focused on the heat center including primary heat exchangers and pump systems. Although the subsystems of the production and consumption fields were concluded in the models, the advanced exergetic evaluations of these systems and the others of GDHS have a lack of investigation. Nevertheless, a GDHS should be evaluated by considering all subsystems such as the production field, geothermal fluid transmitting pipes, network pipelines, substation heat exchangers, and panel radiators of heating circuits for better understanding.

So, in this study, an advanced exergy analysis was conducted, taking the whole system into account. By this integration, it was targeted to determine the upper points of the achievable system since the Pareto principle produces the most compelling part of the operations. Simav GDHS was analyzed by this integrated method to determine endogenous, exogenous, avoidable, and unavoidable parts of the exergy destruction. Finally, the improvement potential of the components and overall system was determined.

2. Material and method

In this study, Simav GDHS was handled for the analysis. Simav GDHS, fed by three production wells located in Simav graben system in Turkey, is currently under operation to heat 5000 residences. The geothermal fluid is obtained from the production wells (EJ-1, EJ-4, and E−11). It is also re-injected through the re-injection well (E−10). The system was installed in 1991 and renewed in 2005 [2]. The flow diagram of the Simav GDHS is given in Fig. 1.

The geothermal wells supply 172 kg/s of geothermal fluid to GDHS. Simav GDHS includes six parts, namely production field (PF), geothermal transmission line (T-line), heat center (C), heating zone transmission line (H-line), substation (S), and heating circuit (HC).

Table 1
A summary of GDHSs.

Study	Explanation	Finding
Arslan et al. [2]	Thermodynamic evaluation of the optimum heating circuit conditions for Simav GDHS.	Exergy efficiency of 43.77% for the optimal condition.
Ozgener et al. [3]	Thermodynamic evaluation of the different GDHDs.	Exergy efficiency from 45.7% to 63.0%.
Kecebas et al. [4]	Thermodynamic evaluation of the Afyon GDHS.	Exergy efficiency of 47.54%.
Yazici [5]	Thermodynamic evaluation of the renovated Afyon GDHS.	Exergy efficiency of 60.63%.
Song et al. [6]	Heat pump integration into GDHS.	A saving of 25.6% on primary heat supply.
Arat and Arslan [7]	Heat pump integration into GDHS.	Exergy efficiency of 76.92% for the optimal design.
Jensen et al. [8]	Heat pump integration into GDHS.	Exergy efficiency of 63.0%.
Sun et al. [9]	Heat pump integration into GDHS.	Exergy efficiency of 61.4%.
Arslan and Kose [10]	Integration of multi-purposed systems including heating of residence, heating of greenhouse, power generation, and balneological use.	Exergy efficiency of 65.75%.
Ghiasirad et al. [11]	Integration of multi-purposed systems including heating, cooling, power generation, desalination, and absorption heat transformer units.	Exergy efficiency of 43.59%.
Ren et al. [12]	Integration of multi-purposed systems including heating and power generation.	Exergy efficiency of 49.73%.

Table 2
Comparative literature review of advanced exergy analysis for GDHSs.

Study	Explanation for unavoidable conditions	Handled subsystem of the GDHS	Exergy efficiency (%)		Increase (%)
			Current	Improved	
Yamankaradeniz [16]	ΔT = 1 °C, η = 0.98, ΔP = 10 kPa	Heat center	25.24	26.34	4.36
Tan and Kecebas [17]	ΔT = 0.5 °C, η = 0.98, ΔP = 10 kPa	Heat center	43.72	45.06	3.07
Kecebas et al. [18]	ΔT = 0.5 °C, η = 0.98, ΔP = 10 kPa	Heat center (Afyon)	27.53	34.72	26.12
		Heat center (Bigadic)	21.03	32.52	54.64
Hepbasli and Kecebas [19]	ΔT = 0.5 °C, η = 0.98, ΔP = 10 kPa	Heat center	29.29	34.46	17.65

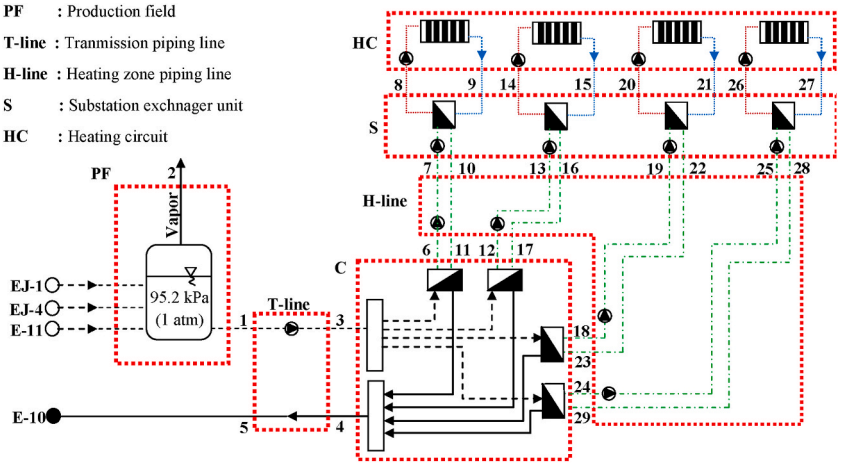

Fig. 1. Flow diagram of Simav GDHS.

The supplied fluid is stored in a tank operating under atmospheric pressure (95.2 kPa). 128.5 kg/s of this mass rate in the liquid phase is fed to GDHS for heating purpose (point 1). The remaining 43.5 kg/s in the gas phase is delivered to the atmosphere (point 2). The fed fluid is later transmitted to the heat center with pre-insulated pipes of 4250 m in length (point 3). After transferring its heat to the circulating water of the heating zone (point 4), the fed fluid is re-injected into the E−10 well (point 5). Finally, the heated circulating water (points 6, 12, 18, and 24) is transferred to substations of the buildings (points 7, 13, 19, and 25) to heat the heating circuit water. There are four heating zones in Simav GDHS. The pipe lengths of the zones are 2250 m, 2200 m, 2000 m, and 1250 m. The heated circuit water (points 8, 14, 20, and 26) transfers its heat to the residence ambient by the aluminum panel radiators with a height of 600

Table 3
Energy balance equations for Simav GDHS.

Components	Energy balance	Efficiency
PF	$\dot{Q}_{loss,PF} = (\dot{m}h_1 + \dot{m}h_2) - (\dot{m}h_{EJ-1} + \dot{m}h_{EJ-4} + \dot{m}h_{E-11})$	$\eta = \frac{\dot{m}h_1 + \dot{m}h_2}{\dot{m}h_{EJ-1} + \dot{m}h_{EJ-4} + \dot{m}h_{E-11}}$
T-line	$\dot{Q}_{loss,T-line} = (\dot{m}h_3 + \dot{m}h_5) - (\dot{m}h_1 + \dot{m}h_4) - \dot{W}_{pump}$	$\eta = \frac{(\dot{m}h_1 + \dot{m}h_4)}{(\dot{m}h_3 + \dot{m}h_5) + \dot{W}_{pump}}$
H-line	$\dot{Q}_{loss,H-line} = (\dot{m}h_7 + \dot{m}h_{13} + \dot{m}h_{19} + \dot{m}h_{25} + \dot{m}h_{11} + \dot{m}h_{17} + \dot{m}h_{23} + \dot{m}h_{29}) - (\dot{m}h_6 + \dot{m}h_{12} + \dot{m}h_{18} + \dot{m}h_{24} + \dot{m}h_{10} + \dot{m}h_{16} + \dot{m}h_{22} + \dot{m}h_{28}) - \dot{W}_{pump}$	$\eta = \frac{(\dot{m}h_7 + \dot{m}h_{13} + \dot{m}h_{19} + \dot{m}h_{25} + \dot{m}h_{11} + \dot{m}h_{17} + \dot{m}h_{23} + \dot{m}h_{29})}{(\dot{m}h_6 + \dot{m}h_{12} + \dot{m}h_{18} + \dot{m}h_{24} + \dot{m}h_{10} + \dot{m}h_{16} + \dot{m}h_{22} + \dot{m}h_{28}) + \dot{W}_{pump}}$
HC	$\dot{Q}_{useful} = (\dot{m}h_9 + \dot{m}h_{15} + \dot{m}h_{21} + \dot{m}h_{27} - \dot{m}h_8 - \dot{m}h_{14} - \dot{m}h_{20} - \dot{m}h_{26}) - \dot{W}_{pump}$	$\eta = \frac{\dot{Q}_{useful}}{(\dot{m}h_8 + \dot{m}h_{14} + \dot{m}h_{20} + \dot{m}h_{26} - \dot{m}h_9 - \dot{m}h_{15} - \dot{m}h_{21} - \dot{m}h_{27}) + \dot{W}_{pump}}$
S	$\dot{Q}_{loss,S} = (\dot{m}h_8 + \dot{m}h_{14} + \dot{m}h_{20} + \dot{m}h_{26} - \dot{m}h_9 - \dot{m}h_{15} - \dot{m}h_{21} - \dot{m}h_{27}) - (\dot{m}h_7 + \dot{m}h_{13} + \dot{m}h_{19} + \dot{m}h_{25} - \dot{m}h_{10} - \dot{m}h_{16} - \dot{m}h_{22} - \dot{m}h_{28}) - \dot{W}_{pump}$	$\eta = \frac{(\dot{m}h_8 + \dot{m}h_{14} + \dot{m}h_{20} + \dot{m}h_{26} - \dot{m}h_9 - \dot{m}h_{15} - \dot{m}h_{21} - \dot{m}h_{27})}{(\dot{m}h_7 + \dot{m}h_{13} + \dot{m}h_{19} + \dot{m}h_{25} - \dot{m}h_{10} - \dot{m}h_{16} - \dot{m}h_{22} - \dot{m}h_{28}) + \dot{W}_{pump}}$
C	$\dot{Q}_{loss,C} = (\dot{m}h_6 + \dot{m}h_{12} + \dot{m}h_{18} + \dot{m}h_{24} - \dot{m}h_{11} - \dot{m}h_{17} - \dot{m}h_{23} - \dot{m}h_{29}) - (\dot{m}h_3 - \dot{m}h_4)$	$\eta = \frac{(\dot{m}h_6 + \dot{m}h_{12} + \dot{m}h_{18} + \dot{m}h_{24} - \dot{m}h_{11} - \dot{m}h_{17} - \dot{m}h_{23} - \dot{m}h_{29})}{(\dot{m}h_3 - \dot{m}h_4)}$
Overall system		$\eta = \frac{\dot{Q}_{useful}}{(\dot{m}h_{EJ-1} + \dot{m}h_{EJ-4} + \dot{m}h_{E-11} - \dot{m}h_5) + \dot{W}_{pump}}$

mm.

2.1. Conventional energy and exergy analysis

In the energy analysis, heat losses ($\dot{Q}_{loss}$) are determined for all the sub-sections of Simav GDHS according to the thermophysical characteristics of the system. Neglecting kinetic and potential energy terms, the mass and energy balances for a component of the system are given as follows;

$$\sum \dot{m}_i - \sum \dot{m}_o = 0 \tag{1}$$

$$\dot{Q} - \dot{W} + \sum \dot{m}_i h_i - \sum \dot{m}_o h_o = 0 \tag{2}$$

where $\dot{Q}$ is the heat rate term, $\dot{W}$ is work term, $\dot{m}$ is the mass rate. i indicates the inlet conditions, and o indicates the outlet conditions. In the energy analysis, all the fluids were assumed as H_2O. Therefore, the energy balance equations are given in Table 3.

The exergy balance for the kth component of the system is given as:

$$\dot{Ex}_k^{Q} - \dot{Ex}_k^{W} - \sum (\dot{m}_i \psi_i)_k - \sum (\dot{m}_o \psi_o)_k - \dot{Ex}_{d,k} = 0 \tag{3}$$

where $\dot{Ex}_k^{Q}$, $\dot{Ex}_k^{W}$, $\dot{Ex}_{d,k}$ and ψ respectively describe the exergy of heat, the exergy of the work, exergy destruction and the specific exergy of flow for the kth component, and are given as:

$$\dot{Ex}_k^{Q} = \left(1 - \frac{T_0}{T}\right) Q_k \tag{4}$$

$$\dot{Ex}_k^{W} = \dot{W}_k \tag{5}$$

$$\psi = (h - h_0) - T_0(s - s_0) \tag{6}$$

Here, h and s indicate orderly enthalpy and entropy at a specific state. Subscript of 0 indicates the reference state conditions. The exergy balance equations for Simav GHDS are given in Table 4.

In Table 2, the overall exergy efficiency was calculated by taking the heat exergy of panel radiators into account since the end product of the system is the heating purpose [23,24].

2.2. Advanced exergy analysis

The essential idea of advanced exergy analysis is based on the endogenous (the exergy destruction occurred within a component

Table 4
Exergy balance equations for Simav GDHS.

Components	Exergy balance	Efficiency
PF	$\dot{Ex}_{d,PF} = (\dot{m}\psi_{EJ-1} + \dot{m}\psi_{EJ-4} + \dot{m}\psi_{E-11}) - (\dot{m}\psi_1 + \dot{m}\psi_2) - \left(1 - \frac{T_0}{T_{ave}}\right)\dot{Q}_{loss,PF}$	$\varepsilon = 1 - \frac{\dot{Ex}_{d,PF}}{(\dot{m}\psi_{EJ-1} + \dot{m}\psi_{EJ-4} + \dot{m}\psi_{E-11})}$
T-line	$\dot{Ex}_{d,T-line} = (\dot{m}\psi h_6 + \dot{m}\psi_{12} + \dot{m}\psi_{18} + \dot{m}\psi_{24} + \dot{m}\psi_{10} + \dot{m}\psi_{16} + \dot{m}\psi_{22} + \dot{m}\psi_{28}) - (\dot{m}\psi_7 + \dot{m}\psi_{13} + \dot{m}\psi_{19} + \dot{m}\psi_{25} + \dot{m}\psi_{11} + \dot{m}\psi_{17} + \dot{m}\psi_{23} + \dot{m}\psi_{29}) + \dot{W}_{pump} - \left(1 - \frac{T_0}{T_{ave}}\right)\dot{Q}_{loss,T-line}$	$\varepsilon = 1 - \frac{\dot{Ex}_{d,T-line}}{(\dot{m}\psi h_6 + \dot{m}\psi_{12} + \dot{m}\psi_{18} + \dot{m}\psi_{24} + \dot{m}\psi_{10} + \dot{m}\psi_{16} + \dot{m}\psi_{22} + \dot{m}\psi_{28}) + \dot{W}_{pump}}$
H-line	$\dot{Ex}_{d,H-line} = (\dot{m}\psi_6 + \dot{m}\psi_{12} + \dot{m}\psi_{18} + \dot{m}\psi_{24} + \dot{m}\psi_{10} + \dot{m}\psi_{16} + \dot{m}\psi_{22} + \dot{m}\psi_{28}) - (\dot{m}\psi_7 + \dot{m}\psi_{13} + \dot{m}\psi_{19} + \dot{m}\psi_{25} + \dot{m}\psi_{11} + \dot{m}\psi_{17} + \dot{m}\psi_{23} + \dot{m}\psi_{29}) + \dot{W}_{pump} - \left(1 - \frac{T_0}{T_{ave}}\right)\dot{Q}_{loss,H-line}$	$\varepsilon = 1 - \frac{\dot{Ex}_{d,H-line}}{(\dot{m}\psi_6 + \dot{m}\psi_{12} + \dot{m}\psi_{18} + \dot{m}\psi_{24} + \dot{m}\psi_{10} + \dot{m}\psi_{16} + \dot{m}\psi_{22} + \dot{m}\psi_{28}) + \dot{W}_{pump}}$
HC	$\dot{Ex}_{d,HC} = (\dot{m}\psi_8 + \dot{m}\psi_{14} + \dot{m}\psi_{20} + \dot{m}\psi_{26} - \dot{m}\psi_9 - \dot{m}\psi_{15} - \dot{m}\psi_{21} - \dot{m}\psi_{27}) + \dot{W}_{pump} + \left(1 - \frac{T_0}{T_{ave}}\right)\dot{Q}_{useful}$	$\varepsilon = 1 - \frac{\left(1 - \frac{T_0}{T_{ave}}\right)\dot{Q}_{useful}}{(\dot{m}\psi_8 + \dot{m}\psi_{14} + \dot{m}\psi_{20} + \dot{m}\psi_{26}) + \dot{W}_{pump}}$
S	$\dot{Ex}_{d,S} = (\dot{m}\psi_7 + \dot{m}\psi_{13} + \dot{m}\psi_{19} + \dot{m}\psi_{25} - \dot{m}\psi_{10} - \dot{m}\psi_{16} - \dot{m}\psi_{22} - \dot{m}\psi_{28}) - (\dot{m}\psi_8 + \dot{m}\psi_{14} + \dot{m}\psi_{20} + \dot{m}\psi_{26} - \dot{m}\psi_9 - \dot{m}\psi_{15} - \dot{m}\psi_{21} - \dot{m}\psi_{27}) + \dot{W}_{pump} - \left(1 - \frac{T_0}{T_{ave}}\right)\dot{Q}_{loss,S}$	$\varepsilon = 1 - \frac{\dot{Ex}_{d,S}}{(\dot{m}\psi_7 + \dot{m}\psi_{13} + \dot{m}\psi_{19} + \dot{m}\psi_{25} - \dot{m}\psi_{10} - \dot{m}\psi_{16} - \dot{m}\psi_{22} - \dot{m}\psi_{28}) + \dot{W}_{pump}}$
C	$\dot{Ex}_{d,C} = (\dot{m}\psi_3 - \dot{m}\psi_4) - (\dot{m}\psi_6 + \dot{m}\psi_{12} + \dot{m}\psi_{18} + \dot{m}\psi_{24} - \dot{m}\psi_{11} - \dot{m}\psi_{17} - \dot{m}\psi_{23} - \dot{m}\psi_{29}) - \left(1 - \frac{T_0}{T_{ave}}\right)\dot{Q}_{loss,C}$	$\varepsilon = 1 - \frac{\dot{Ex}_{d,C}}{(\dot{m}_3\psi_3 - \dot{m}_4\psi_4)}$
Overall system	$\dot{Ex}_{d,total} = \dot{Ex}_{d,PF} + \dot{Ex}_{d,T-line} + + \dot{Ex}_{d,H-line} + \dot{Ex}_{d,HC} + \dot{Ex}_{d,S} + \dot{Ex}_{d,C}$	$\varepsilon = \frac{\dot{Ex}_{useful}}{(\dot{m}\psi_{EJ-1} + \dot{m}\psi_{EJ-4} + \dot{m}\psi_{E-11} - \dot{m}\psi_5) + \dot{W}_{pump,total}}$

depending on its irreversibilities) and exogenous exergy destruction (the exergy destruction occurred within components depending on the irreversibilities of the other component's working conditions). So, the advanced exergy method is a valuable tool for analyzing a whole GDHS. The kth component's exergy destruction essentially forms the sum of the endogenous ($\dot{E}x_{d,k}^{EN}$) and exogenous ($\dot{E}x_{d,k}^{EX}$) exergy destruction terms. It is also the sum of avoidable exergy destruction ($\dot{E}x_{d,k}^{AV}$) and unavoidable exergy destruction ($\dot{E}x_{d,k}^{UN}$). The following equations are used to give the relation between exergy destruction and these terms for the *k*th component [25,26]:

$$\dot{E}x_{d,k} = \dot{E}x_{d,k}^{EN} + \dot{E}x_{d,k}^{EX} \tag{7}$$

$$\dot{E}x_{d,k} = \dot{E}x_{d,k}^{AV} + \dot{E}x_{d,k}^{UN} \tag{8}$$

Splitting the endogenous and exogenous parts into avoidable and unavoidable ones, Eq. (18) can be re-arranged as follows [27]:

$$\dot{E}x_{d,k}^{EN} = \dot{E}x_{d,k}^{EN,AV} + \dot{E}x_{d,k}^{EN,UN} \tag{9}$$

$$\dot{E}x_{d,k}^{EX} = \dot{E}x_{d,k}^{EX,AV} + \dot{E}x_{d,k}^{EX,UN} \tag{10}$$

$$\dot{E}x_{d,k}^{AV} = \dot{E}x_{d,k}^{EN,AV} + \dot{E}x_{d,k}^{EX,AV} \tag{11}$$

$$\dot{E}x_{d,k}^{UN} = \dot{E}x_{d,k}^{EN,UN} + \dot{E}x_{d,k}^{EX,UN} \tag{12}$$

Depending on the splintered exergy destruction, the improvement potential can be calculated by the following equation:

$$IP_k = \frac{\dot{E}x_{d,k}^{AV}}{\dot{E}x_{i,k}} \tag{13}$$

Finally, this modified exergy efficiency can be identified as follows:

Table 5
Thermo-physical characteristics of Simav GDHS for real state.

Points	Fluids	ṁ (kg/s)	T (°C)	P (kPa)	h (kJ/kg)	s (kJ/kgK)
0	H_2O	–	25.00	101.33	104.83	0.3672
EJ-1	Geofluid	72.00	147.70	450.00	1258.52	3.3303
EJ-4	Geofluid	65.00	138.90	350.00	1224.66	3.2861
EJ-11	Geofluid	35.00	88.30	350.00	369.89	1.1731
5	Geofluid	128.50	61.35		256.82	0.8481
1	Geofluid	128.50	98.10		411.16	1.2856
2	Geofluid	43.50	98.10		2672.58	7.3775
3	H_2O	128.50	96.00		402.31	1.2618
4	H_2O	128.50	62.00		259.56	0.8563
6	H_2O	38.40	67.90		284.26	0.9293
7	H_2O	38.40	66.00		276.31	0.9062
8	H_2O	52.94	55.00		230.26	0.7680
9	H_2O	52.94	45.00		188.44	0.6386
10	H_2O	38.40	52.00		217.71	0.7295
11	H_2O	38.40	50.79		212.63	0.7139
12	H_2O	104.20	66.68		279.18	0.9144
13	H_2O	104.20	66.00		276.31	0.9060
14	H_2O	143.66	55.00		230.26	0.7680
15	H_2O	143.66	45.00		188.44	0.6386
16	H_2O	104.20	52.00		217.71	0.7295
17	H_2O	104.20	51.47		215.48	0.7226
18	H_2O	46.60	67.39		282.13	0.9230
19	H_2O	46.60	66.00		276.31	0.9060
20	H_2O	64.25	55.00		230.26	0.7680
21	H_2O	64.25	45.00		188.44	0.6386
22	H_2O	46.60	52.00		217.71	0.7295
23	H_2O	46.60	50.92		213.19	0.7156
24	H_2O	46.60	66.87		279.95	0.9166
25	H_2O	46.60	66.00		276.31	0.9060
26	H_2O	64.25	55.00		230.26	0.7680
27	H_2O	64.25	45.00		188.44	0.6386
28	H_2O	46.60	52.00		217.71	0.7295
29	H_2O	46.60	51.39		215.18	0.7217

$$\varepsilon^{*} = 1 - \frac{\dot{E}x_{d,k} - \dot{E}x_{d,k}^{AV}}{\dot{E}x_{i,k}} \tag{14}$$

Conducting an advanced analysis requires determining the real, ideal, and unavoidable conditions of the components in a system which directly affects the analysis results. In this regard, these conditions should be identified carefully. The pump efficiency of the real case was included in the calculation as 80%, whereas the temperature decrease of the transmission pipes was taken from the measured values. For the unavoidable case, the pump efficiency was assumed to be 90%, whereas the temperature decrease was determined according to the Pareto principle. For the ideal case, pump efficiency and the temperature decrease are 100% and 0 °C, respectively. Keeping the required heat demand of the residences constant, the technical characteristics of Simav GDHS were determined and given in section 2.3 for the real case, section 2.4 for the unavoidable case, and section 2.5 for the ideal case.

2.3. Real conditions

The real conditions are directly related to measured values of the working conditions of the current system. The measured values and thermo-physical characteristics are given in Table 5.

2.4. Unavoidable conditions

The unavoidable conditions depend on the technological parameters most time. It rarely depends on the user definitions for the applications such as insulation. So, there are no limits to identifying the required conditions. In this aim, Pareto principle could be a valuable tool for this kind of analysis. Pareto principle (also referred to as the 80/20 rule) is that 80% of the impact is sourced from the 20% potential cause [28]. Pareto principle is valid for the non-linear changes in many applications, from social issues to industrial ones [29]. According to this idea, it can be assumed that 80% of the heat losses in the transmission pipes can be reduced with an increase of 20% in the insulation thickness. The calculation procedure of the heat losses per unit length that occurred in the pipelines can be given as follows:

$$\dot{q}_{loss} = \frac{2\pi(T_i - T_o)}{\frac{1}{r_1\alpha_i} + \frac{1}{k_{pipe}} ln\left(\frac{r_2}{r_1}\right) + \frac{1}{k_{ins}} ln\left(\frac{r_3}{r_2}\right) + \frac{1}{k_{cover}} ln\left(\frac{r_4}{r_3}\right) + \frac{1}{k_{soil}} ln\left(\frac{r_5}{r_4}\right)} \tag{15}$$

where T_i and T_o indicate the fluid and soil temperatures. The calculations took the soil temperature as 3.4 °C in the calculations [14]. k_{pipe}, k_{ins}, k_{cover}, and k_{soil} are conduction coefficients of pipe material (St-37 steel), an insulation layer (polyurethane), covering material (polyethylene), and soil layer, respectively. These values are taken as 76 W/mK, 0.028 W/mK, 0.43 W/mK and 2.1 W/mK for pipe, insulation, cover and soil, respectively [2,10]. The term r indicated the radius of the pipelayers. In T-line, these values are 0.2 m and 0.2063 m for r_1 and r_2, respectively. The value of r_3 is variable since it defines the thickness of the insulation layer. The value of r_4 is obtained by adding the wall thickness of the cover layer to r_3. The value of r_5 is taken as 0.6 m where the soil temperature is not affected by the heat losses of the pipes [10]. In H-line, these values are 0.15 m, and 0.1552 m for r_1 and r_2, respectively. α_i is the convection coefficient of the fluid and is calculated by:

$$\alpha_i = \frac{Nu \cdot k_{fluid}}{2r_i} \tag{16}$$

where is Nusselt number and given by Ref. [30]:

$$Nu = 0.012\left(Re_D^{0.8} - 280\right)Pr^{0.4} \tag{17}$$

where Pr is Prandtl number taken from Ref. [30]. Re_D is Reynolds number and given in terms of mass flow rate [31]:

$$Re_D = \frac{4\dot{m}}{\mu\pi D} \tag{18}$$

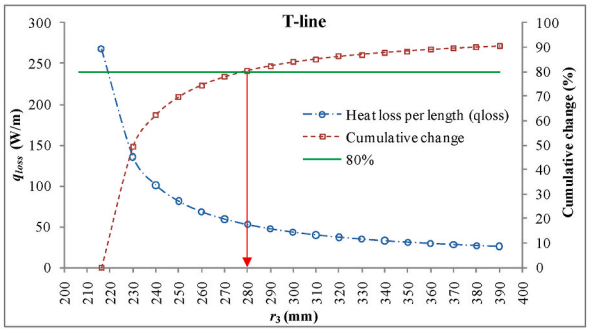

Fig. 2. Pareto result for T-line pipes.

Here μ indicates the dynamic viscosity. Pareto principle was conducted by taking the current status of the pipe structure. In this case, both T-line and H-line pipes have an insulation layer with a thickness of 0.01 m. Heat losses per unit length (q_{loss}) were recorded as approximately 268 W/m and 136 W/m for T-line and H-line, respectively. The variation of heat loss by the thickness of the insulation layer was determined along with the cumulative change. The Pareto point was determined as the value where the cumulative change was 80%. According to this, Pareto evaluations of the pipes are given in Fig. 2 and Fig. 3.

According to Pareto principle, the pre-insulated pipes have a diameter of 560 mm, including stainless steel with a diameter of 400 mm and 6.3 mm wall thickness, polyurethane insulation layer with a thickness of 73.7 mm, and polyethylene cover with a thickness of 6 mm. The pre-insulated pipes have a diameter of 460 mm, including stainless steel with a diameter of 300 mm and 5.6 mm wall thickness, polyurethane insulation layer with a thickness of 74.4 mm, and polyethylene cover with a thickness of 5.2 mm. The heat losses per length unit were determined as 53 W/m and 27 W/m for T-line and H-line, respectively. These Pareto findings are in good agreement with producer values [32]. Also, an insulation addition at a rate of 18.4% and 24.8% of the total diameter of the single steel pipe for respectively T-lines and H-lines brings saving for heat loss at a rate of 80%. These findings also are in good agreement with Pareto principle.

The unavoidable condition for the panel radiators of the heating circuit also depends on the technological parameters. In this equipment, there are no limits to identifying the required conditions. In this regard, Pareto principle seems like a promising approach again. In this study, the inlet temperature of the heating circuit was determined to obtain an increase of 80% in the exergy per unit mass, whereas the outlet temperature was kept constant as in the current (real) status. The exergy change of panel radiators is given in Fig. 4.

According to Fig. 4, the outlet temperature (T_9), keeping the inlet temperature constant at 45 °C, was determined as 61.1 °C, which means an increase of 20% compared to real states. This finding is also in conformity with the Pareto principle. Additionally, the production field was also re-arranged to determine the unavoidable condition. The new configuration is given in Fig. 5.

In Fig. 5, the unused geothermal water (point 1′) is mixed with the heat center's return fluid (point 5). The obtained mixture (point 5′) is then heated by the vapor part (point 2) of the geothermal fluid to obtain the end product of the re-injection (point 5″) well. By doing so, the sustainability of the geothermal reservoir would be increased.

In the analysis, the pump efficiencies were assumed as 90%, where the temperature difference was taken as 5 °C for an effective heat transfer. According to this, the inlet (T_7, T_{13}, T_{19}, and T_{25}) and outlet (T_{10}, T_{16}, T_{22}, and T_{28}) temperatures of S were taken as 66.1 °C and 50 °C. The inlet (T_{11}, T_{17}, T_{23}, and T_{29}) and outlet (T_6, T_{12}, T_{18}, and T_{24}) temperatures of C were determined by considering the Pareto results. The temperature values at the inlet (T_3) and outlet (T_5) of the T-line were also determined according to Pareto results. For the new design of PF, the temperature value is determined via the energy balance equations. The temperature values of points 4, 2', 5', 5" (T_4, $T_{2'}$, $T_{5'}$, *and* $T_{5''}$) were determined via the energy balance equation. Also, all the mass ratios were calculated using the energy balance equation. In the energy balances, it was assumed that all the heat exchangers have an efficiency of 99%. According to these determinations, the unavoidable state characteristics of GDHS are given in Table 6.

2.5. Ideal conditions

The ideal conditions include irreversible conditions. The outlet temperature of HC (T_9, T_{15}, T_{21}, and T_{27}) was also taken at 45 °C for comparative analysis. The pump efficiencies were taken as 100%, whereas the temperature differences were taken as 0 °C. According to these assumptions, the outlet (T_{10}, T_{16}, T_{22}, and T_{28}) temperatures of S and the outlet temperature of C (T_4) were taken as 45 °C. There is no temperature decrease in the T-line and H-line depending on the ideal conditions. So, the inlet (T_3) temperature of C, the outlet (T_6, T_{12}, T_{18}, and T_{24}) temperatures of C, and inlet (T_7, T_{13}, T_{19}, and T_{25}) temperatures of S, were determined as 98.1 °C, whereas the outlet (T_{11}, T_{17}, T_{23}, and T_{29}) temperatures of H-line and the outlet temperature of T-line (T_5) were determined as 45 °C. All the mass ratios and the temperature values of points 2', 5', 5" (T_4, $T_{2'}$, $T_{5'}$, *and* $T_{5''}$) were calculated via the energy balance equations. In the energy balances, it was assumed that all the heat exchangers have an efficiency of 100%. The ideal state characteristics of GDHS are given in Table 7.

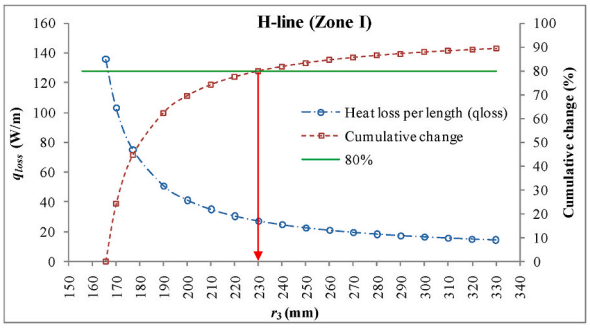

Fig. 3. Pareto result for H-line pipes.

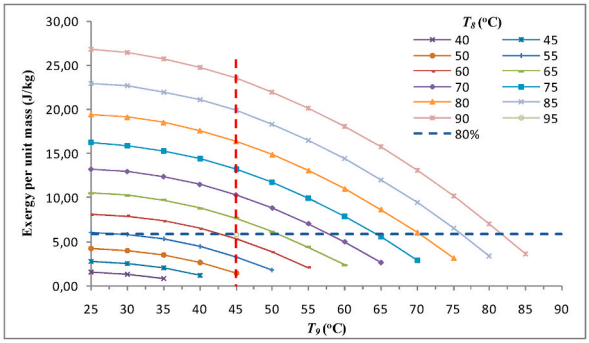

Fig. 4. Pareto result for panel radiators.

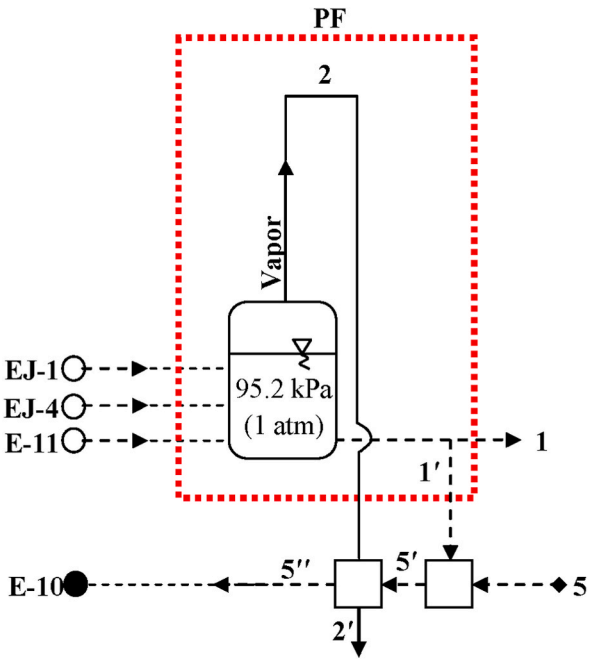

Fig. 5. The new unavoidable (also ideal) configuration of the production field.

3. Results and discussion

In this study, all the subsystems of Simav GDHS were analyzed by the advanced exergy method. Simav GDHS is formed of six subsystems, including production field (PF), transmission piping system (T-line), heat center (C), heating zone piping system (H-line; formed of four zones), substation heat exchanger system (S), and heating circuit system (HC). Firstly, the conventional energy and exergy analysis was conducted for the real system. The results are given in Table 8.

According to Table 8, the most exergy-destructive part of Simav GDHS is the production field with a value of 14362.74 kW and an exergy efficiency of 60.70%. This result is because of the improper management of the geothermal sources with a massive waste of vapor content and heat losses in the field. The second destructive section was determined as the heat exchangers of the heat center with a total exergetic efficiency of 42.31%, which is also the minimum one. The exergetic efficiency of the substation heat exchanger was calculated as 60.03%, which is also relatively lower. These values show that the heat exchanger arrangement still needs to be improved. The H-line and T-line destruction were respectively found as 716.41 kW and 775.91 kW, depending on the higher heat losses from the piping system. The exergetic efficiency of the heating circuit was determined as 49.42%. Finally, the exergetic efficiency of the overall system was determined as 49.64%, which is comparable with the other geothermal district systems in Turkey [3–5]. However, it is clear that it still needs to be rehabilitated on many points. Secondly, the conventional energy and exergy analysis was conducted for the unavoidable system. The results are given in Table 9.

According to Table 9, for the unavoidable state, the most exergy-destructive part of Simav GDHS is still the production field with a value of 12870.17 kW and an exergy efficiency of 64.78%, although the exergy value and efficiency of the resources are increased. This point means there are still much more heat losses at wellheads. The heat center's exergy destruction of heat exchangers was

Table 6
Thermo-physical characteristics of Simav GDHS for the unavoidable state.

Points	Fluids	ṁ (kg/s)	T (°C)	P (kPa)	h (kJ/kg)	s (kJ/kgK)
0	H_2O	–	25.00	101.33	104.83	0.3672
EJ-1	Geofluid	72.00	147.70	450.00	1258.52	3.3303
EJ-4	Geofluid	65.00	138.90	350.00	1224.66	3.2861
EJ-11	Geofluid	35.00	88.30	350.00	369.89	1.1731
1	Geofluid	79.60	98.10		411.17	1.2856
1′	Geofluid	48.90	98.10		411.17	1.2856
2	Geofluid	43.50	98.10		2672.56	7.3773
2′	Geofluid	37.08	98.10		2672.56	7.3773
3	H_2O	79.60	97.44		408.36	1.2781
4	H_2O	79.60	54.82		229.52	0.7657
5	Geofluid	79.60	54.63		228.71	0.7632
5′	Geofluid	128.50	71.19		298.14	0.9695
5″	Geofluid	134.92	98.10		411.1714	1.2856
6	H_2O	33.19	66.54		278.58	0.9126
7	H_2O	33.19	66.10		276.73	0.9072
8	H_2O	32.88	61.10		255.79	0.8450
9	H_2O	32.88	45.00		188.44	0.6386
10	H_2O	33.19	50.00		209.34	0.7038
11	H_2O	33.19	49.67		207.97	0.6995
12	H_2O	90.05	66.26		277.40	0.9092
13	H_2O	90.05	66.10		276.73	0.9072
14	H_2O	89.21	61.10		255.79	0.8450
15	H_2O	89.21	45.00		188.44	0.6386
16	H_2O	90.05	50.00		209.34	0.7038
17	H_2O	90.05	49.88		208.85	0.7023
18	H_2O	40.27	66.42		278.08	0.9112
19	H_2O	40.27	66.10		276.73	0.9072
20	H_2O	39.90	61.10		255.79	0.8450
21	H_2O	39.90	45.00		188.44	0.6386
22	H_2O	40.27	50.00		209.34	0.7038
23	H_2O	40.27	49.76		208.33	0.7007
24	H_2O	40.27	66.30		277.58	0.9097
25	H_2O	40.27	66.10		276.73	0.9072
26	H_2O	39.90	61.10		255.79	0.8450
27	H_2O	39.90	45.00		188.44	0.6386
28	H_2O	40.27	50.00		209.34	0.7038
29	H_2O	40.27	49.88		208.83	0.7022

determined as 686.11 kW with total exergetic efficiency of 66.96%. The exergetic efficiency of the substation heat exchanger was calculated as 72.10%. The H-line and T-line destruction were respectively found as 328.45 kW and 246.31. The exergetic efficiencies are 90.13% and 92.28% in order. The exergetic efficiency of the heating circuit was determined as 64.07%. This point means that it is possible to increase the exergetic value of the panel radiators by regulating the working conditions since there is no chance of reproducing them. Finally, the exergetic efficiency of the overall system was determined as 55.26%. Thirdly, the conventional energy and exergy analysis was conducted for the unavoidable system. The results are given in Table 10.

According to Table 10, for the ideal state, the most exergy-destructive part of Simav GDHS is still the production field with a value of 12475.28 kW and an exergy efficiency of 65.86%, which means that it is not available to increase much more unless the well management is not revised. The exergy efficiency for the heat exchangers of substation heat exchangers was determined as higher as 96.69%, whereas that for the heat center ones was calculated as 100%. The exergetic efficiencies of H-line and T-line destruction were determined as 96.80% and 95.29%, respectively. The exergetic efficiency of the overall system was determined as 60.73%. Finally, the advanced exergy analysis was conducted for Simav GDHS, taking the findings given in Tables 6–8 into account. The results are given in Table 11.

According to Table 11, the highest avoidable exergy destruction ($\dot{E}x_{d,k}^{AV}$) belongs to PF with 1492.58 kW. It means that it is available to avoid exergy destruction at 10.39% by the re-arrangement of PF. In T-line, it is available to avoid the exergy destruction of 529.9 kW by 68.25% in itself. In H-line, it is available to avoid the exergy destruction of 387.96 kW by 54.15% in itself. According to these findings, remarkable exergy destruction could be prevented by applying the Pareto principle for transmission lines. In HC, it is available to avoid the exergy destruction of 89.8 kW by 44.25% in itself. From this point, Pareto rules show that it is also available to prevent exergy destruction at a remarkable rate by just re-arranging the working conditions of the current heating system. In S, it is available to avoid the exergy destruction of 228.12 kW by 34.15% in itself. In C, it is available to avoid the exergy destruction of 933.83 kW by 57.65% in itself. All these destruction values are endogenous ($\dot{E}x_{d,k}^{EN,AV}$) since the exogenous parts ($\dot{E}x_{d,k}^{EX,AV}$) are equal to zero. Accordingly, the subsystems should be recuperated in themselves since the subsystems are not affected by others. The rated distribution of avoidable (AV) and unavoidable (UN) parts of exergy destruction is given in Fig. 6.

According to Fig. 6, the avoidable (AV) exergy destruction part constitutes 8.14% of total exergy destruction, whereas the

Table 7
Thermo-physical characteristics of Simav GDHS for the ideal state.

Points	Fluids	ṁ (kg/s)	T (°C)	P (kPa)	h (kJ/kg)	s (kJ/kgK)
0	H_2O	–	25.00	101.33	104.83	0.3672
EJ-1	Geofluid	72.00	147.70	450.00	1258.52	3.3303
EJ-4	Geofluid	65.00	138.90	350.00	1224.66	3.2861
EJ-11	Geofluid	35.00	88.30	350.00	369.89	1.1731
1	Geofluid	61.04	98.10		411.17	1.2856
1′	Geofluid	67.46	98.10		411.17	1.2856
2	Geofluid	43.50	98.10		2672.56	7.3773
2′	Geofluid	37.49	98.10		2672.56	7.3773
3	H_2O	61.04	98.10		411.17	1.2856
4	H_2O	61.04	45.00		188.44	0.6386
5	Geofluid	61.04	45.00		188.44	0.6386
5′	Geofluid	128.50	72.93		305.3684	0.9907
5″	Geofluid	134.51	98.10		411.1714	1.2856
6	H_2O	9.94	98.10		411.17	1.2856
7	H_2O	9.94	98.10		411.17	1.2856
8	H_2O	9.94	98.10		411.17	1.2856
9	H_2O	9.94	45.00		188.44	0.6386
10	H_2O	9.94	45.00		188.44	0.6386
11	H_2O	9.94	45.00		188.44	0.6386
12	H_2O	26.97	98.10		411.17	1.2856
13	H_2O	26.97	98.10		411.17	1.2856
14	H_2O	26.97	98.10		411.17	1.2856
15	H_2O	26.97	45.00		188.44	0.6386
16	H_2O	26.97	45.00		188.44	0.6386
17	H_2O	26.97	45.00		188.44	0.6386
18	H_2O	12.06	98.10		411.17	1.2856
19	H_2O	12.06	98.10		411.17	1.2856
20	H_2O	12.06	98.10		411.17	1.2856
21	H_2O	12.06	45.00		188.44	0.6386
22	H_2O	12.06	45.00		188.44	0.6386
23	H_2O	12.06	45.00		188.44	0.6386
24	H_2O	12.06	98.10		411.17	1.2856
25	H_2O	12.06	98.10		411.17	1.2856
26	H_2O	12.06	98.10		411.17	1.2856
27	H_2O	12.06	45.00		188.44	0.6386
28	H_2O	12.06	45.00		188.44	0.6386
29	H_2O	12.06	45.00		188.44	0.6386

Table 8
Conventional exergy analysis results for real state.

Components		$\dot{W}$ (kW)	$\dot{Q}$ (kW)	$\dot{E}_i$ (kW)	$\dot{E}_o$ (kW)	$\dot{E}x_i$ (kW)	$\dot{E}x_o$ (kW)	$\dot{E}x_d$ (kW)	η (%)	ε (%)
PF		–	−14070.90	183162.30	169091.40	36546.51	24954.44	14362.74	92.32	60.70
T- line		245	−1733.31	86187.08	84698.77	5322.90	5059.29	775.91	97.99	86.06
H- line	Zone I	30.00	−530.24	19275.51	18775.27	671.66	584.21	171.98	97.25	75.49
	Zone II	110.00	−640.68	51775.45	51244.76	1674.37	1616.95	233.07	98.77	86.94
	Zone III	135.00	−617.02	23292.62	22810.60	766.19	714.03	311.37	98.06	81.18
	Zone IV		−287.59	23190.85	22903.26	753.35	721.91			
	Total	275.00	−2075.54	117534.43	115733.90	3865.56	3637.10	716.41	98.24	82.70
HC	Zone I	32.57	−2214.06	12190.54	9976.48	314.03	313.81	32.78	98.55	49.42
	Zone II	88.38	−6007.93	33079.53	27071.60	852.13	851.54	88.96		
	Zone III	39.53	−2686.85	14793.73	12106.88	381.09	380.83	39.79		
	Zone IV	39.53	−2686.85	14793.73	12106.88	381.09	380.83	39.79		
	Total	200.00	−13595.68	74857.53	61261.84	1928.32	1927.01	201.32		
S	Zone I	42.99	−79.18	2250.24	2214.06	227.21	171.50	106.80	96.55	60.47
	Zone II	116.66	−215.06	6106.33	6007.93	622.96	465.38	296.26	97.70	59.94
	Zone III	52.17	−96.18	2730.85	2686.85	278.60	208.12	132.49	96.86	59.94
	Zone IV	52.17	−96.18	2730.85	2686.85	278.60	208.12	132.49	96.86	59.94
	Total	264.00	−486.59	13818.27	13595.68	1407.37	1053.13	668.05	96.54	60.03
C	Zone I	–	−236.84	2987.32	2750.48	457.26	284.66	208.92	92.07	54.31
	Zone II	–	−1469.21	8106.22	6637.01	1240.80	680.38	785.71	81.88	36.68
	Zone III	–	−412.36	3625.24	3212.88	554.91	330.75	287.39	88.63	48.21
	Zone IV	–	−606.79	3625.24	3018.45	554.91	310.03	337.92	83.26	39.10
	Total	–	−2725.20	18344.01	15618.81	2807.87	1605.83	1619.94	85.14	42.31
Overall system*		***984.00***	***-***	***150160.49***	***13595.68***	***35440.38***	***1051.81***	***18344.37***	***9.00***	***49.64***

Table 9
Conventional exergy analysis results for the unavoidable state.

Components		$\dot{W}$ (kW)	$\dot{Q}$ (kW)	$\dot{E}_i$ (kW)	$\dot{E}_o$ (kW)	$\dot{E}x_i$ (kW)	$\dot{E}x_o$ (kW)	$\dot{E}x_d$ (kW)	η (%)	ε (%)
PF			−14070.22	183162.30	169092.08	36546.51	24955.73	12870.17	92.32	64.78
T- line		134.90	−422.67	50998.39	50710.62	3054.58	3005.17	246.31	97.12	92.28
H- line	Zone I	23.05	−129.91	16192.36	16085.50	530.19	496.22	69.99	99.20	87.35
	Zone II	84.50	−189.02	43832.20	43727.69	1362.72	1352.04	114.05	99.57	92.12
	Zone III	103.71	−198.70	19630.19	19535.20	612.93	603.22	144.42	99.36	89.12
	Zone IV		−54.45	19609.75	19555.30	610.35	604.62			
	Total	211.26	−572.07	99264.50	98903.69	3116.19	3056.11	328.45	99.42	90.13
HC	Zone I	17.98	−2214.06	8409.10	6195.05	279.19	278.89	18.28	99.19	64.07
	Zone II	48.78	−6007.93	22818.45	16810.52	757.60	756.78	49.60		
	Zone III	21.82	−2686.85	10204.79	7517.95	338.81	338.45	22.18		
	Zone IV	21.82	−2686.85	10204.79	7517.95	338.81	338.45	22.18		
	Total	110.39	−13595.68	51637.14	38041.46	1714.41	1712.56	112.24		
S	Zone I	33.03	−55.39	2236.42	2214.06	223.77	190.69	71.64	97.56	72.10
	Zone II	89.62	−150.31	6068.62	6007.93	607.22	517.44	194.40	98.46	72.10
	Zone III	40.08	−67.22	2713.99	2686.85	271.56	231.41	86.94	97.81	72.10
	Zone IV	40.08	−67.22	2713.99	2686.85	271.56	231.41	86.94	97.81	72.10
	Total	202.81	−340.14	13733.01	13595.68	1374.12	1170.94	439.93	97.56	72.10
C	Zone I	–	−23.67	2366.95	2343.28	338.14	234.70	106.91	99.00	68.38
	Zone II	–	−62.36	6235.49	6173.13	917.57	617.90	308.79	99.00	66.35
	Zone III	–	−28.37	2837.35	2808.98	410.35	281.27	133.24	99.00	67.53
	Zone IV	–	−27.96	2796.40	2768.44	410.35	277.28	137.16	99.00	66.57
	Total		−142.36	14236.19	14093.83	2076.42	1411.15	686.11	99.00	66.96
Overall system*		***659.36***	**-**	***127686.00***	***13595.68***	***32160.69***	***1169.10***	***14683.21***	***10.59***	***55.26***

Table 10
Conventional exergy analysis results for the ideal state.

Components		$\dot{W}$ (kW)	$\dot{Q}$ (kW)	$\dot{E}_i$ (kW)	$\dot{E}_o$ (kW)	$\dot{E}x_i$ (kW)	$\dot{E}x_o$ (kW)	$\dot{E}x_d$ (kW)	η (%)	ε (%)
PF		–	−14070.22	183162.30	169092.08	36546.51	24955.73	12475.28	92.32	65.86
T- line		93.10	−93.10	36600.71	36600.71	2148.53	2148.53	105.68	99.32	95.29
H- line	Zone I	6.21	−6.21	5960.42	5960.42	356.10	349.89	13.26	99.90	96.34
	Zone II	22.78	−22.78	16173.85	16173.85	949.43	949.43	25.86	99.86	97.34
	Zone III	27.96	−27.96	7233.22	7233.22	424.60	424.60	31.73	99.81	96.38
	Zone IV			7233.22	7233.22	424.60	424.60			
	Total	56.95	−56.95	36600.70	36600.70	2154.74	2148.53	70.85	99.84	96.80
HC	Zone I	4.89	−2214.06	4087.24	1873.18	323.13	325.77	2.25	99.78	91.15
	Zone II	13.28	−6007.93	11090.89	5082.96	876.82	883.98	6.12		
	Zone III	5.94	−2686.85	4960.03	2273.18	392.13	395.33	2.73		
	Zone IV	5.94	−2686.85	4960.03	2273.18	392.13	395.33	2.73		
	Total	30.04	−13595.68	25098.19	11502.51	1984.20	2000.40	13.84		
S	Zone I	8.90	−8.90	2214.06	2214.06	296.37	296.37	10.11	99.60	96.69
	Zone II	24.16	−24.16	6007.93	6007.93	804.20	804.20	27.42	99.85	96.69
	Zone III	10.80	−10.80	2686.85	2686.85	359.65	359.65	12.26	99.67	96.69
	Zone IV	10.80	−10.80	2686.85	2686.85	359.65	359.65	12.26	99.67	96.69
	Total	54.67	−54.67	13595.68	13595.68	1819.87	1819.87	62.06	99.60	96.69
C	Zone I	–	0.00	2214.06	2214.06	296.37	296.37	0.00	100.00	100.00
	Zone II	–	0.00	6007.93	6007.93	804.20	804.20	0.00	100.00	100.00
	Zone III	–	0.00	2686.85	2686.85	359.65	359.65	0.00	100.00	100.00
	Zone IV	–	0.00	2686.85	2686.85	359.65	359.65	0.00	100.00	100.00
	Total	–	0.00	13595.68	13595.68	1819.87	1819.87	0.00	100.00	100.00
Overall system*		***234.77***	**-**	***127854.77***	***13595.68***	***32174.03***	***1836.08***	***12727.71***	***10.61***	***60.73***

unavoidable (UN) part is about 70.16% for PF. The pairs of AV-UN exergy destruction rates are 2.89%–1.34%, 2.11%–1.79%, 0.49%–0.61%, 1.24%–2.40%, and 5.09%–3.74% for T-line, H-line, HC, S, and C, respectively. The avoidable exergy destruction was calculated as 19.96% for the overall system, whereas the unavoidable part was 80.04%. The rated distribution of endogenous (EN) and exogenous (EX) exergy destruction is given in Fig. 7.

According to Fig. 7, the endogenous exergy destruction part constitutes 10.29% of total exergy destruction, whereas the exogenous part is about 68.01% for PF. The endogenous-exogenous exergy destruction rates are 3.65%–0.58%, 3.52%–0.59%, 1.02%–0.08%, 3.30%–0.34%, for T-line, H-line, HC, and S, respectively. The endogenous exergy destruction part for C is 8.83% and constitutes all of the total exergy destruction of C. The endogenous exergy destruction was calculated as 30.62% for the overall system, while the exogenous was 69.38%. The rated distribution of endogenous avoidable (EN,AV), endogenous unavoidable (EN,UN), exogenous avoidable (EX,AV), and exogenous unavoidable (EX,UN) exergy destructions are given in Fig. 8.

According to Fig. 8, the endogenous avoidable exergy destruction part constitutes 8.14%, 2.89%, 2.11%, 0.49%, 1.24%, and 5.09%, and of total exergy destruction for PF, T-line, H-line, HC, S, and C, respectively. The endogenous avoidable exergy destruction was

Table 11
Advanced exergy analysis results.

Components		$\dot{E}x_{d,k}$	$\dot{E}x_{d,k}^{EN}$	$\dot{E}x_{d,k}^{EX}$	$\dot{E}x_{d,k}^{AV}$	$\dot{E}x_{d,k}^{UN}$	$\dot{E}x_{d,k}^{EN,UN}$	$\dot{E}x_{d,k}^{EX,UN}$	$\dot{E}x_{d,k}^{EX,AV}$	$\dot{E}x_{d,k}^{EN,AV}$
PF		14362.74	1887.46	12475.28	1492.58	12870.17	394.88	12475.28	0.00	1492.58
T- line		775.91	670.23	105.68	529.59	246.31	140.64	105.68	0.00	529.59
H- line	Zone I	171.98	158.71	13.26	101.99	69.99	56.72	13.26	0.00	101.99
	Zone II	233.07	207.21	25.86	119.02	114.05	88.19	25.86	0.00	119.02
	Zone III	311.37	279.64	31.73	166.95	144.42	112.68	31.73	0.00	166.95
	Zone IV									
	Total	***716.41***	***645.56***	***70.85***	***387.96***	***328.45***	***257.60***	***70.85***	***0.00***	***387.96***
HC	Zone I	32.78	30.53	2.25	14.51	18.28	16.02	2.25	0.00	14.51
	Zone II	88.96	82.85	6.12	39.36	49.60	43.48	6.12	0.00	39.36
	Zone III	39.79	37.05	2.73	17.60	22.18	19.45	2.73	0.00	17.60
	Zone IV	39.79	37.05	2.73	17.60	22.18	19.45	2.73	0.00	17.60
	Total	***201.32***	***187.48***	***13.84***	***89.08***	***112.24***	***98.40***	***13.84***	***0.00***	***89.08***
S	Zone I	106.80	96.70	10.11	35.16	71.64	61.54	10.11	0.00	35.16
	Zone II	296.26	268.84	27.42	101.86	194.40	166.98	27.42	0.00	101.86
	Zone III	132.49	120.23	12.26	45.55	86.94	74.68	12.26	0.00	45.55
	Zone IV	132.49	120.23	12.26	45.55	86.94	74.68	12.26	0.00	45.55
	Total	***668.05***	***606.00***	***62.06***	***228.12***	***439.93***	***377.87***	***62.06***	***0.00***	***228.12***
C	Zone I	208.92	208.92	0.00	102.00	106.91	106.91	0.00	0.00	102.00
	Zone II	785.71	785.71	0.00	476.92	308.79	308.79	0.00	0.00	476.92
	Zone III	287.39	287.39	0.00	154.15	133.24	133.24	0.00	0.00	154.15
	Zone IV	337.92	337.92	0.00	200.76	137.16	137.16	0.00	0.00	200.76
	Total	***1619.94***	***1619.94***	***0.00***	***933.83***	***686.11***	***686.11***	***0.00***	***0.00***	***933.83***
Overall system*		***18344.37***	***5616.66***	***12727.71***	***3661.16***	***14683.21***	***1955.50***	***12727.71***	***0.00***	***3661.16***

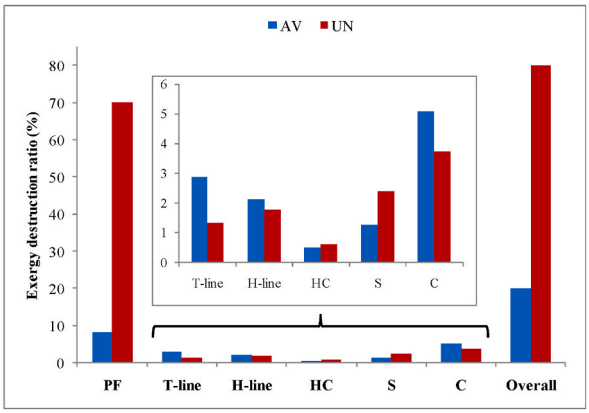

Fig. 6. Percentage distribution of avoidable and unavoidable exergy destructions.

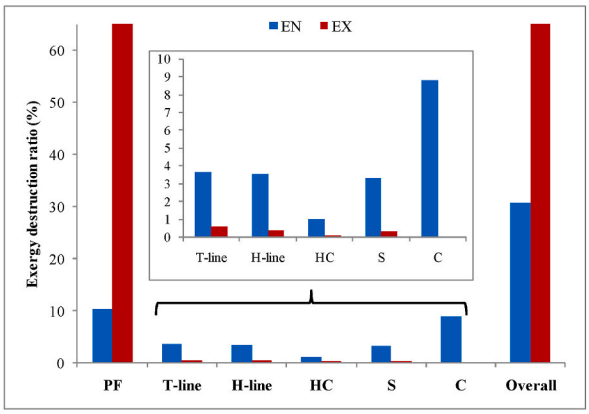

Fig. 7. Percentage distribution of endogenous and exogenous exergy destructions.

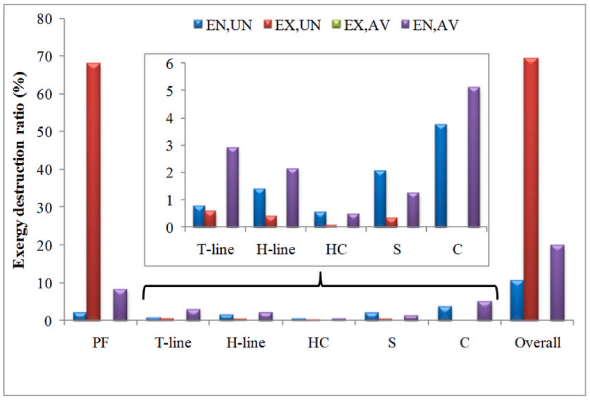

Fig. 8. Rated distribution of endogenous avoidable, endogenous unavoidable, exogenous avoidable, and exogenous unavoidable exergy destructions on the component basis.

calculated as 19.96% for the overall system. The exogenous avoidable exergy destruction part for all components and the overall system equals zero. This means all the units just can be improved by self-rehabilitation, and they are not affected by the working (or design) conditions of the other units, although the working conditions of any component determine those of the connected ones.

Based on the results of advanced exergy analysis, the improvement potentials were determined for each component and overall system. The calculated values are given in Fig. 9. Considering these improvements, the improved exergy efficiencies were calculated as given in Fig. 10.

According to Fig. 9, the improvement potentials were determined as 4.21%, 1.49%, 1.09%, 0.25%, 0.64%, 2.63% and 10.33% for respectively PF, T-line, H-line, HC, S, C and overall system. The greatest improvement was determined for PF depending on the re-arrangements of waste heat recovery of vapor content which also affects the overall system. Just applying rehabilitation in an amount of 20% in the T-line, H-line, and HC according to Pareto principle, it is available to achieve an improvement of about 2.84%.

According to Fig. 10, the maximum efficiency increase was recorded for C with an improved exergy efficiency of 75.56%, whereas the real one is about 42.31%. On the other hand, the improved exergy efficiency of PF is recorded as 64.78%, whereas that of the real state is 60.70%. For the overall system, the improved efficiency was recorded as 58.57%, with an increase of 17.99% compared to the real state. This value is comparable with the literature given in Table 2. Moreover, it is more realistic and achievable in terms of Pareto approach.

From the sustainability point of view, the most critical subsystem comes into prominence as PF, with the highest exergy destruction of 14,362.74 kW. So, by a simple rehabilitation of PF including the re-arrangements of waste heat recovery of vapor content, it is possible to reduce this destruction down to 12,870.17 kW. This process would definitively increase the lifetime of the geothermal reservoirs. However, there are still remarkable losses that can be gained by different integrated application techniques such as electricity generation, greenhouse heating, and cooling with low-temperature. The heat losses that occurred in the transmission lines (T-line and H-line) are another prominent problem that also could be prevented by technical processes such as insulation. In the current status (real case), this issue causes an exergy destruction of 1492.32 kW. Also, this destruction causes a temperature decrease of about 0.5 °C per km, which directly affects the GDHS. According to Pareto principle, it is possible to decrease this destruction down to 574.77 kW by adequate insulation. One of the essential structures of the heating of buildings is the heating circuit, including the panel radiators. In the current system with 55/45 °C, the exergy destruction is recorded as 231.32 kW, which is relatively lower in comparison

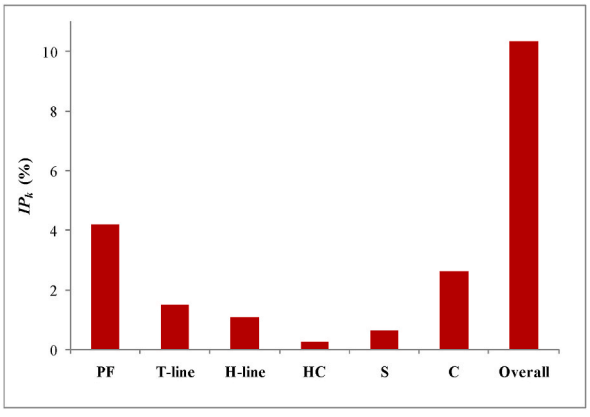

Fig. 9. Improvement potentials.

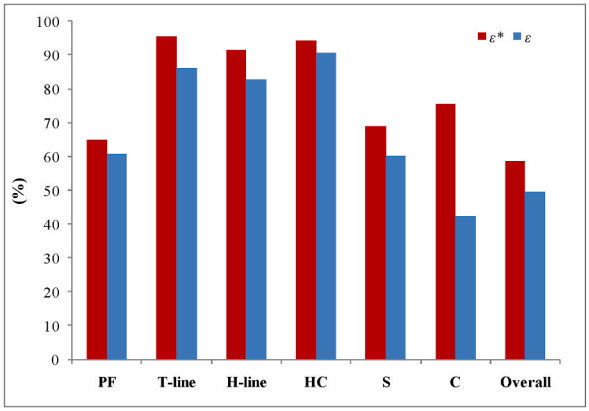

Fig. 10. Exergy and improved exergy efficiencies.

to other subsystems. However, just re-arranging the circuit as 61.1/45 °C in the lights of Pareto principle, it is possible to decrease the exergy destruction down to 112.24 kW, although the required heat demand is kept constant. The main parameter in this decrease is the mass flow rate, fluid properties, and pump efficiency.

4. Conclusion

In this study, advanced exergy analysis was conducted to perform the improvement ability of Simav GDHS, considering all subunits. Since there is no limit for the transmission lines and heating circuit, the unavoidable conditions were determined by integrating Pareto principle into the advanced exergy method. The following main findings were concluded:

- Technically available unavoidable cases were identified by Pareto's idea. It was also very suitable and in good agreement with the energy (district heating) systems.
- The most exergy-destructive part of GDHS was determined as PF. Although the available rehabilitation conditions were applied (unavoidable and real states), it was still the most exergy-destructive part. The improvement potential was determined as 4.21%. All the improvement potential comes from endogenous rehabilitations. So, resource management is an urgent need since it is impossible to change the source characteristics.
- Also, the exogenous avoidable exergy destruction was determined as zero for all parts. This means all the improvements should individually be conducted for the parts of GDHS.
- The improvement potential of heat exchangers of C was found as 2.63%, whereas it was 1.33% for the overall system. According to this, it is available to increase the efficiency of C up to 75.76% with an increase of %78.59. On the other hand, this rate is about 14.51% for the heat exchangers of S. Also, it is possible to increase the exergy efficiency of the overall system up to 58.57%, with an increase of 17.99% in comparison to the current status.
- It was found that it is available to increase the exergetic efficiency of the panel radiator (heating circuit) by an amount of 4.02% compared to the current status just by the change of working conditions.
- The available increase in exergy efficiency of T-line was found at 10.82%. This rate is about 10.64% for H-line.

Declaration of competing interest

The authors declare that they have no known competing financial interests or personal relationships that could have appeared to influence the work reported in this paper.

Nomenclature

$\dot{E}$	energy rate (kW)
$\dot{Ex}$	exergy rate (kW)
h	specific enthalpy (kJ/kg)
I	exergy destruction rate (kW)
IP	improvement potential (%)
k	conductive heat transfer coefficient (W/mK)
$\dot{m}$	mass flow rate (kg/s)
P	pressure (kPa, bar, or atm)
Pr	Prandtl number
$\dot{q}$	heat rate per length (kW/m)
$\dot{Q}$	heat rate (kW)

r	Radius (m)
Re	Reynolds number
s	specific entropy (kW/kgK)
T	temperature (K or ^{o}C)
$\dot{W}$	work rate (kW)

Greek symbols

α	convective heat transfer coefficient (W/m^{2}K)
ε	exergy efficiency (%)
η	energy efficiency or isentropic efficiency (%)
μ	dynamic viscosity (Ns/m^2)
ψ	specific flow exergy (kJ/kg)

Subscripts

d	destruction
D	diameter
i	inlet or ith component
ins	insulation
k	kth component
o	outlet
T	value at a specified temperature
0	value at the reference state

Superscripts

Q	exergy term related to heat
W	exergy term related to work
o	standard
EX	exogenous
EN	endogenous
AV	avoidable
UN	unavoidable
*	modified

Abbreviations

C	Centre of heat (or Heat center)
GDHS	Geothermal district heating system
HC	Heating circuit
H-line	Heating zone transmission line
PF	Production field
S	Substation
T-line	Geothermal zone transmission line

References

[1] J.W. Lund, A.N. Toth, Direct utilization of geothermal energy 2020 worldwide review, Geothermics 90 (2021), 101915.
[2] O. Arslan, M.A. Ozgur, R. Kose, A. Tugcu, Exergoeconomic evaluation on the optimum heating circuit system of Simav geothermal district heating system, Energy Build. 41 (2009) 1325–1333.
[3] L. Ozgener, A. Hepbasli, I. Dincer, A key review on performance improvement aspects of geothermal district heating systems and applications, Renew. Sustain. Energy Rev. 11 (2007) 1675–1697.
[4] A. Keçebas, M. Kayfeci, E. Gedik, Performance investigation of the Afyon geothermal district heating system for building applications: exergy analysis, Appl. Therm. Eng. 31 (2011) 1229–1237.
[5] H. Yazici, Energy and exergy based evaluation of the renovated Afyon geothermal district heating system, Energy Build. 127 (2016) 794–804.
[6] Z. Song, N. Wang, S. You, Y. Wang, H. Zhang, S. Wei, X. Zheng, J. Guo, Integration of geothermal water into secondary network by absorption-heat-pump-assisted district heating substations, Energy Build. 202 (2019), 109403.
[7] H. Arat, O. Arslan, Exergoeconomic analysis of district heating system boosted by the geothermal heat pump, Energy 119 (2017) 1159–1170.
[8] J.K. Jensen, T. Ommen, W.B. Markussen, B. Elmegaard, Design of serially connected district heating heat pumps utilising a geothermal heat source, Energy 137 (2017) 865–877.
[9] F. Sun, B. Hao, L. Fu, H. Wu, Y. Xie, H. Wu, New medium-low temperature hydrothermal geothermal district heating system based on distributed electric compression heat pumps and a centralized absorption heat transformer, Energy 232 (2021), 120974.
[10] O. Arslan, R. Kose, Exergoeconomic optimization of integrated geothermal system in Simav, Kutahya. Energy Conversion and Management 51 (2010) 663–676.
[11] H. Ghiasirad, N. Asgari, R.K. Saray, S. Mirmasoumi, Thermoeconomic assessment of a geothermal based combined cooling, heating, and power system, integrated with a humidification-dehumidification desalination unit and an absorption heat transformer, Energy Convers. Manag. 235 (2021), 113969.

[12] C. Ren, J. Wang, H. Chen, X. Liu, M. An, Thermodynamic analysis and comparative investigation of a new combined heating and power system driving by medium-and-high temperature geothermal water, Energy Convers. Manag. 233 (2021), 113914.
[13] G. Manente, A. Lazzaretto, I. Molinari, F. Bronzini, Optimization of the hydraulic performance and integration of a heat storage in the geothermal and waste-to-energy district heating system of Ferrara, J. Clean. Prod. 230 (2019) 869–887.
[14] D.I. Stanica, M. Bachmann, M. Kriegel, Design and performance of a multi-level cascading district heating network with multiple prosumers and energy storage, Energy Rep. 7 (2021) 128–139.
[15] Y. Chen, H. Hua, J. Wang, P.D. Lund, Thermodynamic performance analysis and modified thermo-ecological cost optimization of a hybrid district heating system considering energy levels, Energy 224 (2021), 120067.
[16] N. Yamankaradeniz, Thermodynamic performance assessments of a district heating system with geothermal by using advanced exergy analysis, Renew. Energy 85 (2016) 965–972.
[17] M. Tan, A. Kecebas, Thermodynamic and economic evaluations of a geothermal district heating system using advanced exergy-based methods, Energy Convers. Manag. 77 (2014) 504–513.
[18] A. Kecebas, C. Coskun, Z. Oktay, A. Hepbasli, Comparing advanced exergetic assessments of two geothermal district heating systems for residential buildings, Energy Build. 81 (2014) 141–151.
[19] A. Hepbasli, A. Kecebas, A comparative study on conventional and advanced exergetic analyses of geothermal district heating systems based on actual operational data, Energy Build. 61 (2013) 193–201.
[20] M. Ucar, O. Arslan, Assessment of improvement potential of a condensed combi boiler via advanced exergy analysis, Therm. Sci. Eng. Prog. 23 (2021), 100853.
[21] O. Arslan, M.S. Acar, Enhanced exergetic evaluation of regenerative and recuperative coal-fired power plant, Int. J. Exergy 35 (2021) 263–289.
[22] O. Arslan, O. Erbas, Investigation on the improvement of the combustion process through hybrid dewatering and air pre-heating process: a case study for a 150 MW coal-fired boiler, J. Taiwan Inst. Chem. Eng. 121 (2021) 229–240.
[23] O. Arslan, M.A. Ozgur, H.D. Yildizay, R. Kose, Fuel effects on optimum insulation thickness: an exergetic approach, Energy Sources, Part A Recovery, Util. Environ. Eff. 32 (2010) 128–147.
[24] A. Avşar, O. Arslan, Thermodynamic analysis of the heating concept for a residence, BSEU Journal of Science 7 (2020) 80–90, https://doi.org/10.35193/bseufbd.706281.
[25] S. Kelly, G. Tsatsaronis, T. Morosuk, Advanced exergetic analysis: approaches for splitting the exergy destruction into endogenous and exogenous parts, Energy 34 (2009) 384–391.
[26] G. Tsatsaronis, M.H. Park, On the avoidable and unavoidable exergy destructions and investment costs in thermal systems, Energy Convers. Manag. 43 (2002) 1259–1270.
[27] T. Morosuk, G. Tsatsaronis, Advanced exergetic evaluation of refrigeration machines using different working fluids, Energy 34 (2009), 2548-2458.
[28] Milan V. Pareto, Manuale di Economia politica. Piccola biblioteca scientifica, English Translation by, in: A. Schwier, Manual of Political Economy Kelley Publishers, New York, 1906, 1971.
[29] R. Koch, The 80/20 Principle: the Secret of Achieving More with Less, Nicholas Brealey Publishing Ltd., London, 1998.
[30] H. Yuncu, S. Kakac, Basic Heat Transfer, Bilim Publishing Ltd., Ankara, 1999 (in Turkish).
[31] J. Nagao, S. Matsuo, T. Setoguchi, H.D. Kim, Numerical study on the effect of unsteady downstream conditions on hydrogen gas flow through a critical nozzle, Open J. Fluid Dynam. 2 (2012) 137–144.
[32] Data for pre-insulated pipes, Available from: (in Turkish.) Last Access: March 14th, http://jeoterm.com.tr/index.php/service/seri-1-izolasyon-olculeri/, 2022.